Heat Transfer and Flow Structure Evaluation of a Synthetic Jet Emanating from a Planar Heat Sink

Paul Manning[1], Tim Persoons[1], Nick Jeffers[2], Brian Donnelly[2], Darina Murray[1]

[1]Mechanical and Manufacturing Engineering, Parsons Building, Trinity College, Dublin 2, Ireland
[2]Bell Labs Ireland, Blanchardstown Industrial Estate, Dublin 15, Ireland

E-mail: manninp@tcd.ie

Abstract. Direct impinging synthetic jets are a proven method for heat transfer enhancement, and have been subject to extensive research. However, despite the vast amount of research into direct synthetic jet impingement, there has been little research investigating the effects of a synthetic jet emanating from a heated surface, this forms the basis of the current research investigation. Both single and multiple orifices are integrated into a planar heat sink forming a synthetic jet, thus allowing the heat transfer enhancement and flow structures to be assessed. The heat transfer analysis highlighted that the multiple orifice synthetic jet resulted in the greatest heat transfer enhancements. The flow structures responsible for this were identified using a combination of flow visualisation, thermal imaging and thermal boundary layer analysis. The flow structure analysis identified that the synthetic jets decreased the thermal boundary layer thickness resulting in a more effective convective heat transfer process. Flow visualisation revealed entrainment of local air adjacent to the heated surface; this occurred from vortex roll-up at the surface of the heat sink and from the highly sheared jet flow. Furthermore, a secondary entrainment was identified which created a surface impingement effect. It is proposed that all three flow features enhance the heat transfer characteristics of the system.

1. Introduction

Over the past decade, heat dissipation in microprocessors has more than doubled [1]. The trend of electronic device miniaturization and increasing power density results in very high localised heat fluxes, this presents a thermal bottleneck in the electronics component cooling sector [2]. The basic requirement for a thermal management system is to efficiently dissipate heat from a heated surface to ensure safe operating conditions, as thermal overstressing is one of the major causes for failure of electronic devices [3]. However, as form factors of electronic devices decrease in size, there is an increase in the demand for confined space thermal management solutions.

Synthetic jets have been at the forefront of electronic component cooling research for the past number of years. The two stroke motion of a synthetic jet results in the periodic ejection and suction of a working fluid across an orifice, creating vortex roll-up at the surface of the orifice and subsequent vortex ejection into the surrounding flow field. Conventional synthetic jets create a train of vortices which impinge onto a heated surface resulting in enhanced heat transfer characteristics. The strength

and size of the vortex ejected from the synthetic jet cavity is determined by the dimensionless stroke length, L_0/D, where the stroke length L_0 is determined by the following expression:

$$L_0 \int_0^{\frac{\tau}{2}} u_m(t)dt = \frac{2U_0}{f} \quad (1)$$

where U_o is the average ejection velocity from the orifice and f is the forcing frequency. The dimensionless stroke length can be defined as L_0/D and is inversely proportional to the Strouhal number, therefore $\frac{L_o}{d} = \frac{1}{2}\left(\frac{fd}{U_o}\right)^{-1}$. This relationship determines the characteristics of the synthetic jet flow, since the stroke length parameter governs vortex detachment at the orifice [10]. The following criterion must be satisfied for vortex detachment from a sharp edged orifice of a synthetic jet, $\frac{L_o}{d} > 0.5$ [10] as below this threshold vortex rings do not escape the orifice and are re-entrained back into the cavity on the suction phase, resulting in reduced heat transfer [6]. For $2.56 < \frac{L_o}{d} < 8.9$ the vortices increase in size, and there is virtually no interaction between successive vortices [11]. Increasing the vortex strength will therefore increase the volumetric entrainment of the surrounding flow field; this has a positive effect on heat transfer due to the increased mass flux. Another method which increases the volumetric flow entrainment is by integrating multiple in-phase synthetic jets. Research conducted by Chaudari et al. [3] identified that the heat transfer coefficient for multiple synthetic jets is up to 30% higher as compared to that obtained with a conventional single orifice synthetic jet at the same excitation frequency. This heat transfer enhancement is attributed to the increase in fresh fluid entrainment resulting from the increased entrainment rates.

Current research into synthetic jets focusses on parameters such as stroke length [6,7,9], orifice to impingement surface distance [6,7,9], flow confinement and recirculation [4], orifice geometries [5] and multiple orifices [3]. However, this investigation evaluates the heat transfer characteristics of single and multiple synthetic jets *emanating* from a heated surface. It is hypothesised that the synthetic jet flow will periodically break down the thermal boundary layer and promote localised turbulence generation and mixing at the surface of the heat sink. Additionally, heated air from the thermal boundary layer is expected to be entrained into the synthetic jet and ejected from the surface. The heat transfer analysis provides an insight into the average Nusselt number resulting from the synthetic jet actuation. Through additional heat transfer analysis, the relative heat transfer contribution from the upper and lower surfaces of the heat sink is also identified. The overall heat transfer resulting from jet actuation is examined for a single orifice and multiple orifices and flow structures responsible for the heat transfer enhancements are identified using three flow structure analysis methods; flow visualisation, thermal imaging and thermal boundary layer analysis.

2. Experimental Set-up and Procedure

The unique feature about the heat sink design is that the synthetic jet is part of the heated surface, whereas conventionally synthetic jets direct cooler air at a heated surface. The ejection plate channels the flow by forcing the enclosed air through an orifice thus creating a synthetic jet. By attaching an oscillating diaphragm onto the base of the heat sink, a synthetic jet flow can be created. Two synthetic jet heat sink configurations are created for the heat transfer and flow structure analysis; a single orifice and a 2 X 2 array of orifices with a centre-to-centre spacing, Z, of 15 mm. The diameter for each orifice, d, is 5 mm as shown in *figure 1*. The multiple orifice heat sink therefore has a Z/d ratio of 3. Heat is provided by four cartridge heaters which fit into machined holes on the side of the heat sink. Pressure recovery slots are machined into the sides of the heat sink perpendicular to each heater slot to alleviate any difficulty associated with cartridge heater removal. Thermocouple grooves are machined into the upper and lower surface of the heat sink fitted with T-type thermocouples, to measure the heat sink temperature. Copper is the preferred material for the heat sink design for its excellent thermal conductivity, creating an isothermal boundary condition. Thermal imaging results indicated that the heat sink surface has a temperature deviation of 0.9℃ for a surface heat sink

temperature of 74℃, with the highest temperature variation occurring at the heat sink/insulation interface. Both heat sink designs are depicted in *figure 1*.

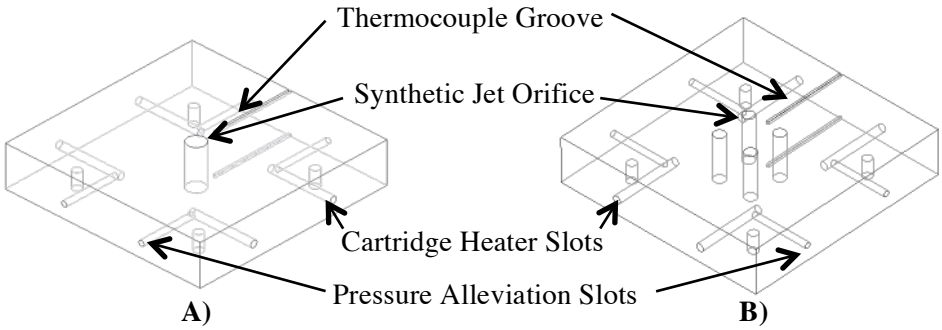

Figure 1. Copper heat sink designs A) Single orifice and B) Multiple orifices

The synthetic jet was generated using an electro mechanically driven actuator i.e. an acoustic speaker. An acoustic cavity, with embedded pressure microphone is used to measure the pressure generated by the speaker within the chamber. The inner diameter of the acoustic cavity conforms to the 71.5 mm diameter of the speaker ensuring no flow disruptions, which could affect the pressure measurements. The pressure measurements are used to calculate the Reynolds number and stroke length for the synthetic jet flow through the orifice. This was achieved using Persoons and O'Donovan [12] cavity pressure method for synthetic jet velocity estimation.

The experimental set-up was designed to minimize thermal conduction losses through the system. This was achieved using low thermal conductivity (~0.023 $\frac{W}{m.K}$) insulation. A cross section of the synthetic jet test section is shown in *figure 2*.

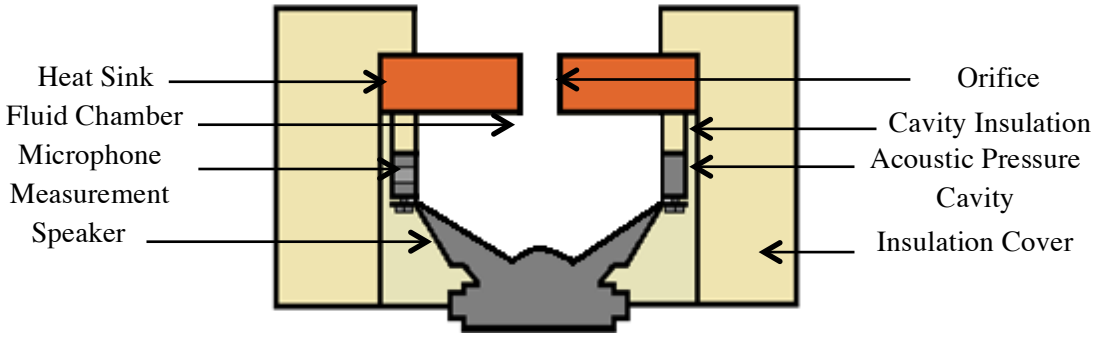

Figure 2. Schematic of synthetic jet set-up

4. Experimental Procedure

4.1 Heat Transfer

The cartridge heaters supply the copper heat sink with a constant power of 4 W via an HP 6033A power system supply (0 – 20 V / 0 – 20 A, 200 W). The Visaton FRS 8 speaker is actuated using LabView software which controls the amplitude and frequency of a sine wave output to a signal amplifier. The amplified signal is then passed into the speaker, which actuates the speaker diaphragm creating a synthetic jet through the heat sink orifice. Temperature measurements are taken on the upper and lower surfaces of the heat sink, inside the jet cavity, in the ambient air and at the base of the speaker. Once the temperature of the heat sink reaches steady-state, the temperatures, Reynolds number, Stroke Length and pressure are all recorded. The Reynolds number is calculated by the following expression:

$$Re = \frac{U\,d}{\nu} \quad (2)$$

where U is the jet velocity, d is the orifice diameter and ν is the kinematic viscosity of air. For the multiple orifice case, the diameter of a single orifice (i.e. 5 mm) is used; therefore, the Reynolds number represents the jet flow through a single orifice. The testing procedure is repeated for a variety of frequencies and stroke lengths. The multiple orifice heat sink was tested at the same stroke length twice with two different speakers identifying repeatability of the test and assessing the influence of the speaker characteristics. The maximum variation between both data sets for Nusselt number and Reynolds number is 5.2% and 5.6% respectively.

The novel implementation of a synthetic jet integrated into a heat sink increases the complexity of the heat transfer analysis. Synthetic jet actuation will enhance the heat transfer from the heat sink, however, quantifying how much of the heat transfer enhancement is a direct result of jet actuation requires accounting for the system losses. The main losses which must be investigated are: conduction through the insulation housing, Q_{cond}, radiative heat losses from the surface of the heat sink, Q_{rad}, and the additional heat added to the copper heat sink induced from the heat generated due to ohmic heating in the voice coil driver in the loudspeaker, Q_{add}. The convective heat transfer is therefore a function of these parameters, as shown in following equation:

$$Q_{Total} = Q_{heater} + Q_{add} - Q_{cond} - Q_{rad} \quad (3)$$

Once the system losses have been accounted for, the heat transfer coefficient, h, is calculated from:

$$h = \left(\frac{Q_{Total}}{A\Delta T}\right) \quad (4)$$

where Q_{Total} is defined above [W], h is the heat transfer coefficient $\left[\frac{W}{m^2 k}\right]$, A is the area exposed to the jet flow [m^2] and ΔT is the temperature difference between the surface heat sink temperature and ambient temperature [K]. The average Nusselt number, $\overline{Nu}$, for mixed convection is calculated as:

$$\overline{Nu}_{mix} = \left(\frac{h\,L_{char}}{k}\right) \quad (5)$$

where k is the thermal conductivity $\left[\frac{W}{mk}\right]$ and L_{char} is the length scale for the heat sink surface.

The Nusselt number defined by the experimental measurements incorporates natural convection from the heat sink. Therefore in order to obtain a representative Nusselt number for the synthetic jet actuation alone, natural convection heat transfer must be accounted for. The influence of natural convection on the total heat transfer is described by the following relationship:

$$Nu_{mix}{}^3 = Nu_{Forced}{}^3 + Nu_{Natural}{}^3 \rightarrow Nu_{Forced} = \left(Nu_{mix}{}^3 - Nu_{Natural}{}^3\right)^{\frac{1}{3}} \quad (6)$$

The direct heat transfer enhancements resulting from synthetic jet actuation is represented by the forced nusselt number.

4.2 Flow Visualisation

Flow visualisation was implemented to capture high speed images of the synthetic jet flow. Flow visualisation operates by injecting seeding particles into the flow field, so that it describes the same flow pattern as the jet flow [13]. The particles can be visualised using a laser sheet and camera. The laser sheet was orientated vertically and positioned at the centre of the orifice. The camera was positioned perpendicular to the laser sheet, as depicted in *figure 3*. The camera and laser are controlled using LaVision software. The sample rate of the camera is slightly lower than the actuation frequency of the jet, therefore capturing vortex propagation over many periods. The seeding medium is introduced to the synthetic jet system and is highlighted by the laser allowing the identification of the flow features generated by the synthetic jet. The post processing of the results was undertaken using the LaVision software.

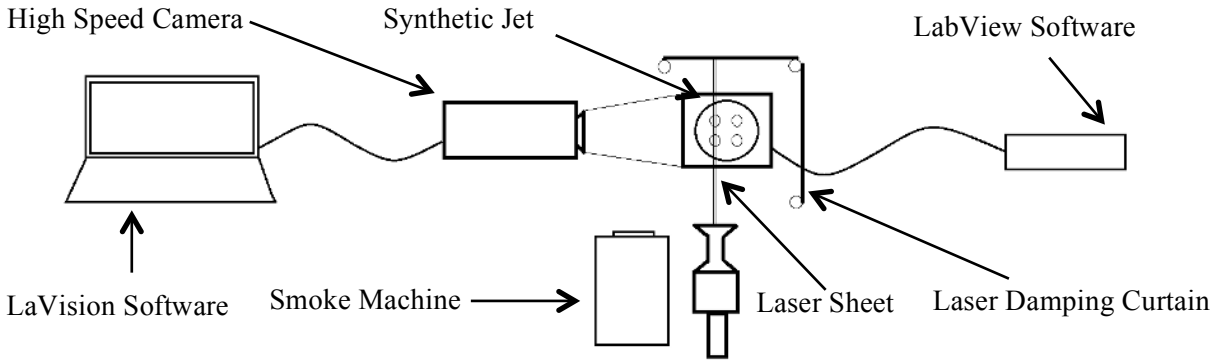

Figure 3. Schematic of the flow visualisation experimental set-up

4.3 Thermal Imaging

Thermal imaging gives another visual representation of the effects of the synthetic jet flow structures on surface heat transfer. The thermal imaging camera was mounted onto a tripod and orientated vertically downward, the heat sink was positioned underneath camera. The experimental set-up for the thermal imaging procedure is depicted in *figure 5*. The emissivity of the heat sink surface was experimentally obtained by in camera comparison to a reference thermocouple. The analysis and post processing was undertaken using FLIR software.

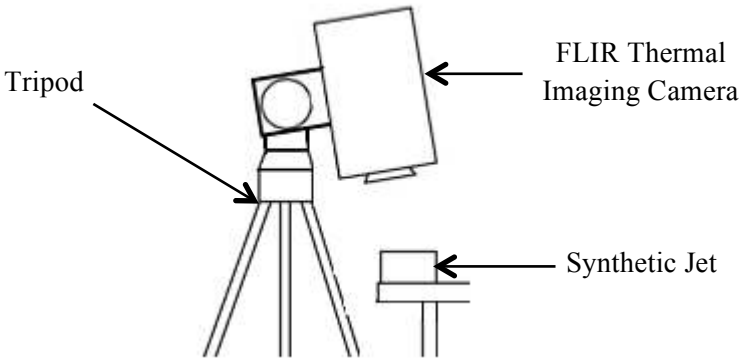

Figure 5. Schematic of the thermal imaging experimental set-up

4.4 Temperature/Boundary Layer Analysis

To establish a thermal boundary layer profile for the heat sink, temperature measurements were taken at and directly above the heat sink surface. Four measurement points which were identified along the radius of the multiple orifice heat sink as indicated in *figure 6 A)*. These are located at:

1) the edge of the insulation
2) 15 mm from the insulation edge
3) between the multiple orifice pair
4) at the centre of the heat sink

The temperature measurements recorded above the measurement positions were taken at 1 mm increments from 1 mm 10 mm above the heat sink, in 2 mm increments from 10 mm to 20 mm and 5 mm increments from 20 mm to 70 mm above the heat sink. This was done for natural convection and synthetic jet conditions. The experimental set-up is depicted in *figure 6 B)*.

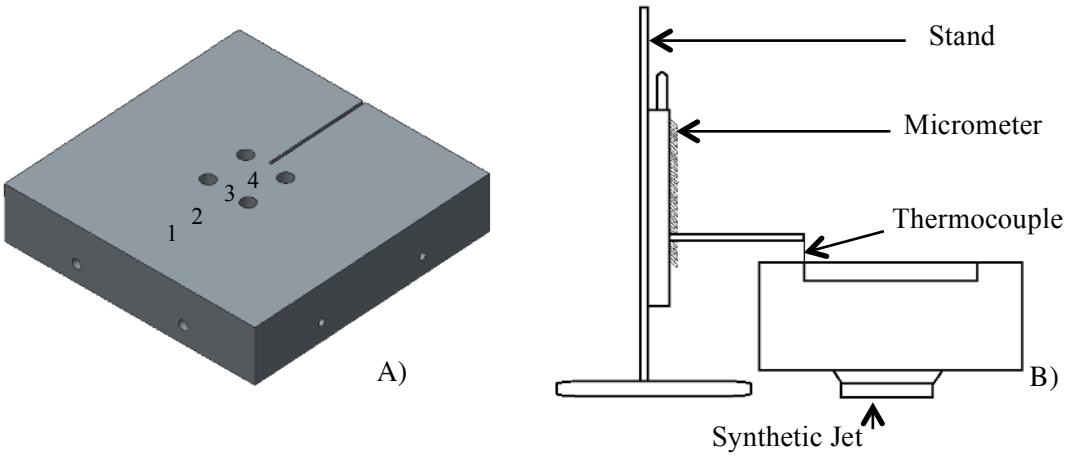

Figure 6. A) Temperature measurements used for boundary layer analysis, B) Schematic of the thermal boundary layer experimental set-up

5. Results and Discussion

5.1.Heat Transfer Analysis

Firstly, the single orifice heat sink was assessed with synthetic jet flow as a function of frequency. The total heat transfer was calculated, this included the heat transfer from the upper and lower surfaces of the heat sink. The results indicate that increasing the frequency of actuation, increases the rate of heat transfer in general. A higher frequency range was tested for the lower stroke length of 2.5, this indicated in a peak in heat transfer at 350 Hz, after which the heat transfer decreases as shown in *figure 7*. This may be due to a cavity resonant frequency or a harmonic of the resonant frequency at 350 Hz. The rate of heat transfer also increases substantially as the stroke length of the synthetic jet is increased, this is a consequence of an increase in the volumetric flow rate. As the volumetric flow rate through the orifice increases, the entrainment of the surrounding flow field is also increased. The jet flow becomes highly sheared increasing the rate of entrainment. This process is hypothesised to decrease the boundary layer thickness, reducing the temperature gradient between the surface and ambient.

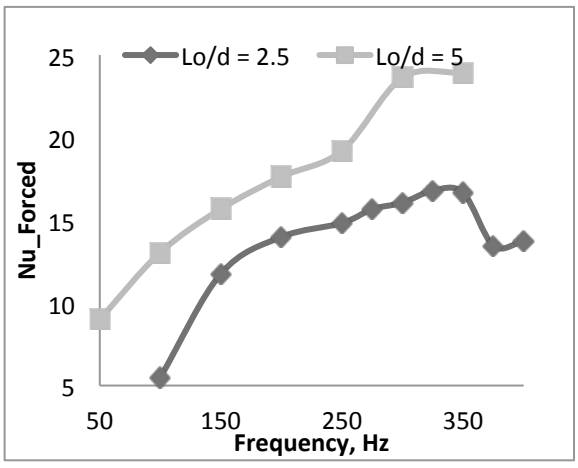

Figure 7. Frequency dependence on heat transfer for a single orifice at stroke lengths of 2.5 and 5

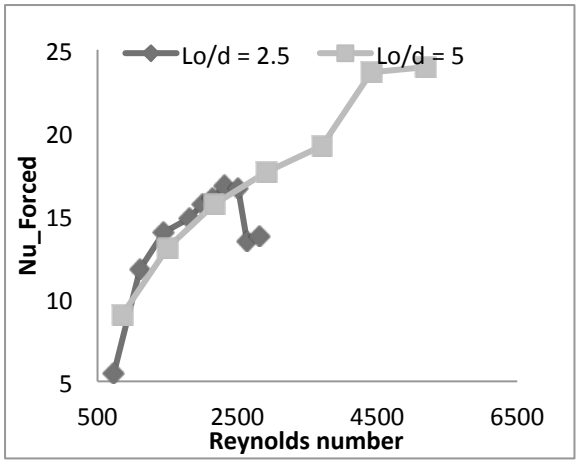

Figure 8. Reynolds number dependence on heat transfer for a single orifice at stroke lengths of 2.5 and 5

The dimensionless stroke lengths used during testing ensures that the vortex generated at the orifice detaches from the surface and is not re-ingested back into the cavity. To avoid the re-ingested process the minimum stroke length tested was 2.5, which is above the sharp edge orifice criterion for vortex

detachment of $\frac{L_o}{d} > 0.5$ [10]. The higher stroke length substantially increases the rate of heat transfer, which has also been identified in the literature for direct synthetic jet impingement [6, 7, 14].

The heat transfer analysis on the single orifice also highlighted that the greatest heat transfer enhancement occurs at the upper surface of the heat sink. Both upper and lower surfaces were insulated, in turn, and the heat transfer enhancements for both surfaces were analysed. The results are presented in *figure 9*.

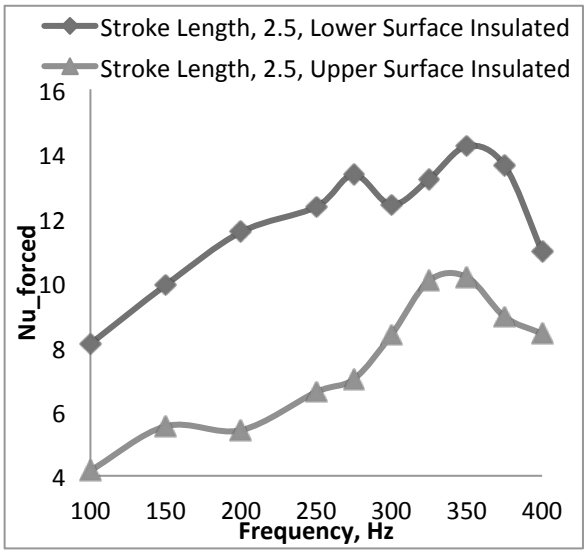

Figure 9. Comparison of heat transfer between the upper surface to the lower surface heat sinks at a constant stroke length of 2.5

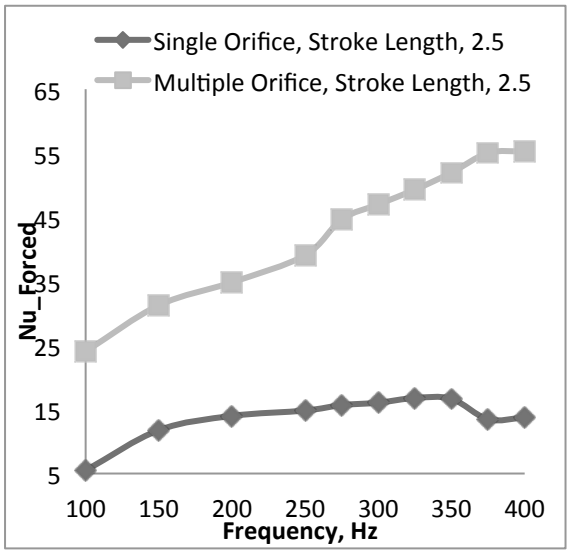

Figure 10. A comparison between the heat transfer of a single orifice and a multiple orifice heat sink at a constant stroke length of 2.5

Figure 9 indicates that the trends between both datasets are similar achieving peak heat transfer at 350 Hz. However, as the excitation frequency is increased the heat transfer on the lower surface increases at a higher rate compared to the upper surface. The physical cause of this is yet unknown and will require further investigation.

The multiple orifice heat sink resulted in a significantly larger heat transfer enhancement compared to the single orifice heat sink. The significant increase in heat transfer coincides with results found by Chaudari et al. [3] for multiple orifice impinging synthetic jets. However, a more significant finding in this research was that the increase in the number of orifices increased the volumetric entrainment of the surrounding flow field, this would indicate why the heat transfer is significantly higher. The difference in heat transfer between the single and multiple orifice heat sink is evident in *figure 10*. The peak heat transfer for the multiple orifice heat sink occurs at a higher frequency than for the single orifice, this may be due to the change in resonant frequency of the synthetic jet cavity or the increase in surface area due to extra orifices. The results obtained indicate that the frequency and Reynolds number increase linearly, therefore a Nusselt number correlation at a set stroke length is obtained. The Nusselt number corrections are presented in *Table 1*.

Table 1. Nusselt number correlations for single and multiple orifice synthetic jet actuation

Nusselt Number Correlations				
Jet Type	*Stroke Length*	*Reynolds Number*	*Correlation*	R^2
Multiple Orifice	2.5	750 < Re < 3,000	$0.6987\ Re^{0.5443}$	0.9831
Single Orifice	2.5	1,100 < Re < 2,500	$0.5877\ Re^{0.4309}$	0.9703
Single Orifice	5	750 < Re < 5,500	$0.2522\ Re^{0.5344}$	0.986

5.2. Flow Structure

The multiple orifice heat sink resulted in the highest heat transfer enhancement of all the orifice configurations tested, therefore the flow structures developed by the multiple orifice heat sink were investigated. The analysis of these flow structures is presented in *figure 11*.

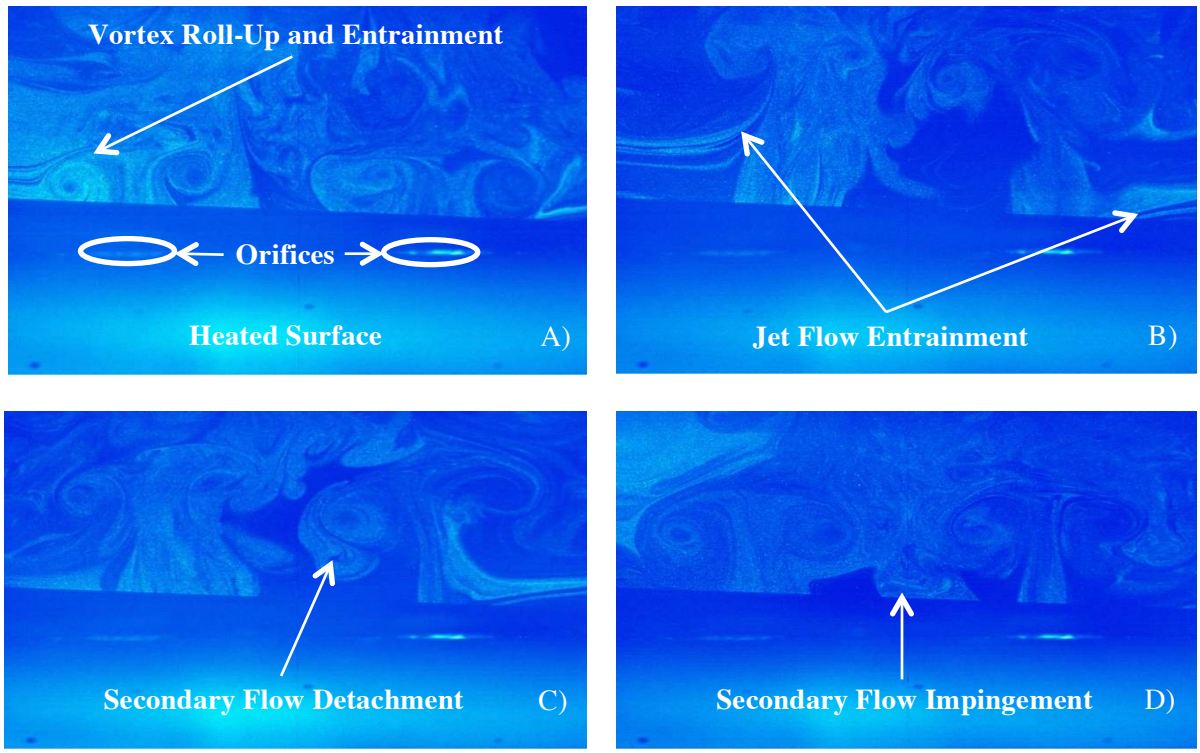

Figure 11. Flow visualisation of the multiple orifice heat sink at a stroke length of 5 A) Vortex Roll-Up, B) Jet Flow Entrainment, C) Secondary Flow Detachment and D) Secondary Flow Impingement

Vortex formation initiates at the edge of the orifice as the top of the fluid slug is ejected from the cavity. The vortex continues to roll-up during the ejection phase until it is finally advected downstream. This process is depicted in *figure 11 A)* which identifies vortex roll-up at the surface of the orifice, this is typical behaviour for a synthetic jet. The image provides sufficient evidence to indicate that local turbulence generation and flow field entrainment is occurring, again satisfying one of the initial hypotheses as a method responsible for increasing heat transfer. The figure also depicts both vortices rolling up simultaneously, which indicates that both of the synthetic jets are in phase, as expected.

The high momentum ejection stroke of the synthetic jet creates a highly sheared jet flow, these shear layers entrain the surrounding ambient flow, breaking down the thermal boundary layer. However, it is not only during vortex roll-up that the highly sheared flow entrains the ambient flow; entrainment induced by the jet flow as the vortex is advected downstream is also evident in *figure 11*

B). While the vortex is advected downstream, the synthetic jet is drawing the surrounding air into the cavity during the suction phase. During this period of ejection, the jet flow is entraining the surrounding flow field above the heat sink surface, while the cavity is entraining the flow field at the surface of the heat sink. The dual entrainment process is depicted in *figure 11 B)*. Both entrainment methods are assumed to increase the heat transfer by continually breaking down the thermal boundary layer at the heat sink surface.

Boundary layer entrainment and vortex induced turbulence are not the only methods of cooling which have been identified when analysing the multiple orifice heat sink. A differential pressure induced impingement was identified as a by-product from the propagating jet flow. A sub pressure zone is generated as both vortices become detached from the orifices. These propagating vortices entrain the surrounding flow field in the direction of ejection, which increases the volumetric flow rate of the jet. However, the entrainment of the fluid between the orifice pair creates a sub pressure zone. The counter rotating vortices at the top of the jet column entrain the fluid between both jet streams, this entrained fluid then detaches from the vortex by the differential pressure between the jet flow and sub pressure zone. This secondary entrainment forces the ambient flow in the opposing direction of ejection, and subsequently impinges on the surface of the heat sink. These jet flow characteristics are highlighted in *figure 11 C)* and *D)*. To identify the velocity and vorticity of the secondary entrainment, P.I.V. analysis must be conducted, this is planned for the second phase of this research.

5.3 Thermal Boundary Layer Analysis

The cooling method of the synthetic jet device was hypothesised to be a result of thermal boundary layer break-up. This results from the entrainment of the ambient flow field and local turbulence generation around orifice edge. The thermal boundary layer which is assumed to be diminished is analysed using this thermal boundary layer investigation. The results of the analysis are presented in *figures 12* and *13*.

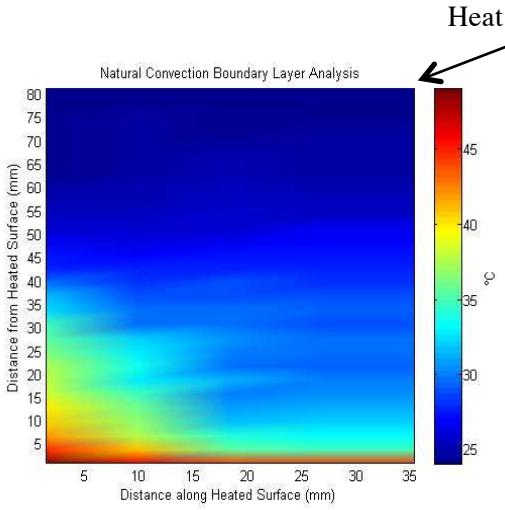

Figure 12. Thermal boundary layer analysis of the multiple orifice heat sink from natural convection

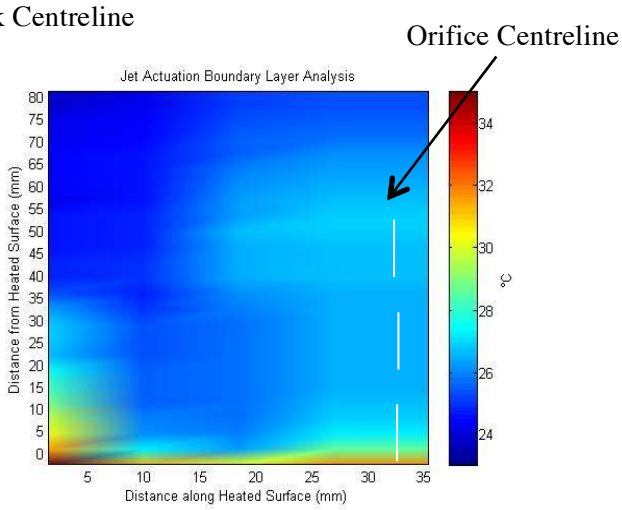

Figure 13. Thermal boundary layer analysis of the multiple orifice heat sink from jet actuation

Figures 12 and *13* illustrate the temperature of the air occurring at the edge of the insulation, which is a result of the increased temperature of the heat sink underneath the insulation; this is also identified in the thermal imaging analysis. The boundary layer thickness for the natural convection analysis is highest at the edge of the insulation and is subsequently cooled along the length of the heat sink, which contrasts to conventional natural boundary layer development. This can be attributed to the high local temperatures at the heat sink/insulation interface. *Figure 13* illustrates the effect of

synthetic jet actuation on the thermal boundary layer tempertaure. The figure indicates that the synthetic jet successfully disrupts the thermal boundary layer over the surface of the heat sink, satisfying the initial cooling process hypothesis.

6. Conclusion

An investigation into the heat transfer and flow structure developed by a synthetic jet emanating from a heat sink was undertaken. The heat transfer analysis provided sufficient evidence to indicate that a multiple orifice synthetic jet provided the greatest heat transfer enhancements, with the upper surface of the heat sink providing the greater heat transfer contribution. The flow structures responsible for the heat transfer enhancements were also identified using flow visualisation. The enhanced heat transfer characteristics resulted from boundary layer thinning from ambient flow field entrainment.

Acknowledgements

The authors acknowledge the technical staff of the Mechanical and Manufacturing Engineering Department in Trinity College Dublin and the industry sponsor Bell Labs Ireland.

References

[1] M. Baelmans, R. Gielen, T. Persoons, F. Rogiers, T. Saenen, T. Oevelen, Optimization of Convective Heat Transfer in Micro-Scale Electronics Cooling Applications, Houille Blanche-Revue Internationale De L'Eau, 66 (2011), 70 – 78

[2] S. V. Garimella, L-T. Yeh, T. Persoons, Thermal Management Challenges in Telecommunication Systems and Data Centres, IEEE Transactions on Components, Packaging and Manufacturing Technology, 2 (2012), 1302 – 1326

[3] M. Chaudhari, B. Puranik, A. Agrawal, Multiple Orifice Synthetic Jet for Improvement in Impingement Heat Transfer, International Journal of Heat and Mass Transfer, 54 (2011), 2056 – 2065

[4] T.L. Lupton, D.B. Murray, A.J. Robinson, The Effects of Varying Confinement Levels on the Heat Transfer to a Miniature Impinging Air Jet, 5th European Thermal-Sciences Conference, paper no. Jet 5, Eindhoven, 2008.

[5] M. Chaudari, B. Puranik, A. Agrawal, Effect of Orifice Shape in Synthetic Jet Based Impingement Cooling, Experimental Thermal and Fluid Science, 34 (2010), 246 – 256

[6] R. Farrelly, A. McGuinn, T. Persoons, D. B. Murray, Heat Transfer Behaviour and Flow Field Characterisation of Impinging Synthetic Jets for a Wide Range of Parameters, Proceedings of the International Heat Transfer Conference (2010), Washington D.C.

[7] M. Chaudari, B. Puranik, A. Agrawal, Heat Transfer Characteristics of Synthetic Jet Impingement Cooling, International Journal of Heat and Mass Transfer, 53 (2010), 107 – 1069

[8] T. McGuinn, A Study of the Heat Transfer Process and Related Flows of a Synehtic Jet Impinging Perpendicular to a Heated Surface, A thesis submitted to the University of Dublin (2011)

[9] A. Glezer, M. Amitay, Synthetic Jets, Annual Review of Fluid Mechanics, 34 (2002), 503 -529

[10] T. Persoons, General reduced-Order Model to Design & operate Synthetic Jet Actuators, AIAA Journal, 50 (2012), 916 - 927

[11] R. Holman, Y. Utturkar, R. Mittal, B. L. Smith, L. Cattafesta, Formation Criterion for Synthetic Jets, AIAA Journal, 43 (2005), 2110 - 2116

[12] T. Persoons, T. S. O'Donovan, A Pressure-Based Estimate of Synthetic Jet Velocity, Physics of Fluids, 19 (2007), 128104

[13] C. Carcasci, An Experimental Investigation on Air Impinging Jets using Visualisation Methods, International Journal of Thermal Science (1999) 38, 808 – 818

[14] R. Farrelly, A. McGuinn, T. Persoons, D. B. Murray, A Heat Transfer Comparison between a Synthetic Jet and a Steady Jet at Low Reynolds Number, Proceedings of 2008 ASME International Mechanical Engineering Congress (2008), 505 – 510